Subject-Specific and Strain-Rate-Dependent Material Modeling of Human Femurs for Dynamic Loading

Ankit Malik, Ved Vyas Yadav, Sanjeev Lalwani, Rajesh Malhotra, Anoop Chawla, Naresh V. Datla

Abstract Long bone injuries often result from trauma, necessitating prolonged rehabilitation that significantly affects daily activities. Accurate finite element (FE) models are crucial for understanding bone behaviour under impact. However, prior strain-rate-dependent models treated bone as homogeneous, lacking subject-specific material properties. The objective of this work is to optimise a subject-specific and strain-rate-dependent material model for the human femur that can predict the structural response over a range of impact velocities. Human femur samples were tested under dynamic three-point bending at impact velocities of 1.5 m/s, 3.0 m/s, and 5.0 m/s. Subject-specific FE mesh of the specimen was obtained using CT scans and heterogenous material mapping was performed based on Hounsfield Number. A bilinear strain-rate-dependent material model was developed that incorporates the rate dependency of yielding and pre- and post-yield behaviour of bone using a user-defined material model in LS-DYNA™. The material model parameters were optimised to minimise deviation from the experimental force-time response using a genetic algorithm-based inverse FE characterisation. A single material model was thus obtained that reasonably predicts the structural response in all cases. Cortical bone's quasi-static elastic modulus ranged from 7.5 to 19.3 GPa, and quasi-static yield stress varied from 63 to 118 MPa.

Keywords Dynamic three-point bend, genetic algorithm, human femur, inverse characterisation, strain-rate-dependent.

I. INTRODUCTION

Long bone trauma frequently occurs during accidents and sports activities [1], with the femur and tibia being the most frequently fractured due to high-energy impacts [2-3]. These fractures often necessitate lengthy rehabilitation, significantly affecting a patient's ability to perform daily activities [4]. Finite Element (FE) models have proven essential for understanding bone behaviour under impact [5-6], but their accuracy depends on robust numerical models capable of capturing bone's dynamic response.

Previously proposed strain-rate-dependent models have treated bone as a homogeneous material without subject-specific material property assignment [7]. However, the literature presents a wide range of material properties [8], and subject-specific material property assignment is known to increase the accuracy of the material models [9-11]. The objective of this work is to derive a subject-specific and strain-rate-dependent material model for the human femur that can predict the structural response over a range of impact velocities.

II. METHODS

Experimental Testing

Three human femurs were obtained from un-embalmed post-mortem human subjects (PMHS) aged 40–60 years from the All India Institute of Medical Sciences (AIIMS) and Jai Prakash Narayan Apex Trauma Centre, New Delhi, following approval from their standing ethics committee, and were subjected to dynamic three-point bending tests. Samples were frozen at -20°C and were thawed to room temperature before testing, and all soft tissues were removed. All the bones were scanned using a micro-CT scanner (Scanco XtremeCT II™, Scanco Medical AG, Switzerland). The CT data were used to develop subject-specific finite element (SSFE) models and to determine the specimens' geometric properties.

To prevent the rotation of the bone from the intended impact direction, both extremities of the bone were potted in hollow aluminum mounts using quick-setting bone cement (Poly Methyl Methacrylate, PMMA). Dynamic three-point bend tests were performed utilising a custom-built drop tower apparatus (Fig. 1) [12]. A

A. Malik (tel: +91 9711460737; e-mail: ankitmalik.iyf@gmail.com) is a PhD student, V. V. Yadav is a Project Scientist, and A. Chawla and N. V. Datla are Professors in the Department of Mechanical Engineering at the Indian Institute of Technology (IIT) Delhi, India. S. Lalwani is a Professor in the Department of Forensic Science and Toxicology, All India Institute of Medical Sciences, New Delhi, India. R. Malhotra is a Professor in the Department of Orthopaedics, All India Institute of Medical Sciences, New Delhi, India.

piezoelectric load cell (Dytran 1053V6, Hottinger Brüel & Kjaer, United Kingdom) was fixed between the crosshead and the impactor to measure the load during the impact event. The potted femur specimens were positioned freely on the cylindrical roller support fixtures with a bending span of 200 mm, as illustrated in Fig. 1. The femurs were impacted at the mid-shaft (impactor weight 30.5 kg) at velocities of 1.5 m/s, 3.0 m/s, and 5.0 m/s in the lateral to medial direction until failure. A high-speed digital camera (MotionPro® Y-Series) was used to record the displacement of the impactor and crack propagation. An external triggering mechanism was employed using a thin copper tape to initiate and synchronise the data acquisition system and high-speed digital camera recording.

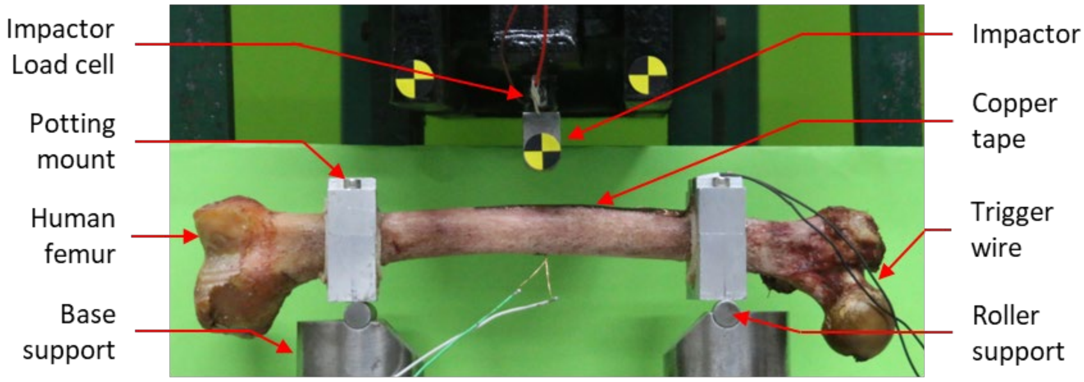

Fig. 1. Custom-built drop tower apparatus used for performing dynamic three-point bend test on human femur.

Computational Modeling

CT images of bones were processed using Mimics® 24.0 (Materialise, Leuven, Belgium). The preliminary segmentation employed a grayscale threshold filter. The segmented model was carefully refined using manual editing, region growing, and erasing tools. Subsequent to surface mesh generation, HyperMesh (v. 2022, Altair Engineering, Inc., USA) was employed to create a tetrahedral volumetric mesh, which was further refined.

The volumetric SSFE meshes were imported into Mimics to assign isotropic heterogeneous material properties based on grey-scale information obtained from CT scan data. A linear relationship was established between Hounsfield units (HU) and bone apparent density (ρ) using the standardised hydroxyapatite phantom (Q1 Scanco phantom). According to the HU values, bone apparent density was divided into 100 distinct material bins based on [13]. To replicate the experimental setup, SSFE models were first exported to HyperMesh and then imported into the LS-DYNA™ solver, and boundary conditions were applied for conducting finite element (FE) simulations (model is illustrated in Fig. 2).

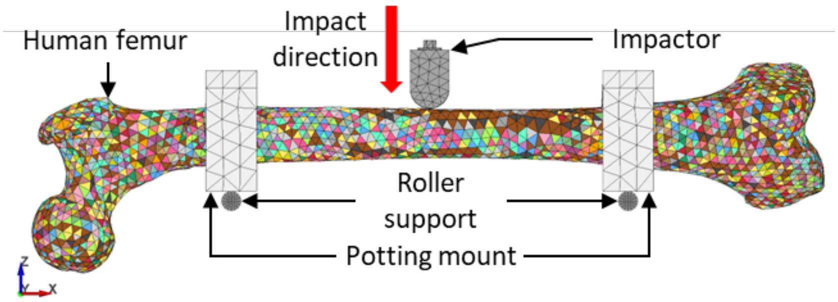

Fig. 2. LS-DYNA™ SSFE model replicating the dynamic three-point bend test of human femur.

Strain-rate-dependent Material Model

In this study, trabecular bone was modeled using a bilinear elastic-plastic material. The initial parametric sensitivity analysis indicates that trabecular bone minimally affects the dynamic response of bone under three-point bending. Therefore, its material properties (Table I) were adopted from [14], with only the cortical bone's material properties characterised in this study. The existing elastic-plastic constitutive model (MAT_24) in LS-

DYNA™ solely accounts for strain-rate effects on yield stress. Therefore, an elastic-plastic strain-rate-dependent model was implemented using the user-defined material (UMAT) model in LS-DYNA™ to incorporate strain-rate dependency of pre- and post-yield behaviour of bone.

For each element, quasi-static elastic modulus (E_0) and yield stress (σ_{y0}) were mapped using the power law relationships in accordance with the assigned ρ value (Equations 3 and 5). Previous studies reported correlations, including exponential, logarithmic, and polynomial functions, to address the implementation of strain-rate dependency [12][15-16]. In this study, the strain-rate-dependent elastic modulus (E) and yield stress (σ_y) were obtained using a combined exponential and logarithmic function (Equations 4 and 6), based on the quasi-static strain rate ($\dot{\varepsilon}_0$) and the target strain rate ($\dot{\varepsilon}$). A von Mises criterion was used to capture yielding. The tangent modulus (E_t) was taken to be a factor 't' times the strain-rate-dependent elastic modulus (E), as shown in Equation 7. In this study, the fracture phenomenon of bone is not considered, therefore only the pre-fracture behaviour is modeled, and simulations are conducted until the time when fracture is observed in the tests. The material parameters shown in Table II were optimised using the inverse FE methodology.

TABLE I
MATERIAL PROPERTIES OF TRABECULAR BONE

Young's modulus (GPa)	Poisson's ratio	Yield stress (GPa)	Tangent modulus (GPa)	Cowper Symonds model parameters
0.445	0.3	0.0053	0	C = 0 & P = 0

Inverse FE characterisation

In this study, the genetic algorithm (GA)-based inverse FE optimisation was implemented using the GA toolbox in MATLAB (version R2022b, MathWorks, Inc.). The material parameters are altered iteratively using the optimisation method to reduce the error between simulation and experimental force response. The variation between the experimental and SSFE force-time responses for individual impact velocity was determined using a normalised root mean square error function ($NRMS^j$) (Equation 1).

$$NRMS^j = \sqrt{\frac{1}{n^j}\sum_{i=1}^{nj}\left(\frac{F_i^{fem,j} - F_i^{exp,j}}{max.(F_i^{exp,j})}\right)^2}, \forall j = 1 \ to \ 3 \tag{1}$$

where the $F_i^{exp,j}$ and $F_i^{fem,j}$ are the experimental and FE force values corresponding to the individual impact velocity (j); the index j corresponds to the different impact velocities (1.5 m/s, 3.0 m/s, and 5.0 m/s); and n_j is the number of data points according to the corresponding test. The root mean square error function is normalised using the maximum experimental force value ($max.(F_i^{exp,j})$) corresponding to the specific impact velocity. The objective function for the GA is the summation of uniformly weighted $NRMS$ values for all individual velocities, as expressed in Equation 2.

$$\text{Objective function, } f : \ min \ NRMS^{total} = \sum_{j=1}^{3} NRMS^j \tag{2}$$

A single set of optimised material model parameters was obtained that can reproduce the force response from 1.5 m/s to 5.0 m/s. The design parameters and their range used in the overall optimisation study are presented in Table II.

III. RESULTS

The peak load at failure varied with impact velocity and was measured to be 4.7 kN, 6.78 kN, and 3.27 kN for 1.5 m/s, 3.0 m/s, and 5.0 m/s, respectively (see Fig. 4). Fracture initiation times decreased with increasing velocity, recorded as 2.6 ms, 1.8 ms, and 1.0 ms. The initial force-time slope showed a velocity-dependent trend, peaking at 10.63 kN/ms for 5.0 m/s and dropping to 3.62 kN/ms for 1.5 m/s. Oblique fractures were observed in all experiments.

Force-time data and SSFE models were used to optimise material parameters by minimising the objective function of Equation 2. Objective function convergence (Fig. 3) occurred by the 9th iteration, with a slight fall at the 18th iteration (objective function value: 0.281). Simulations (Fig. 4) show a reasonable agreement with experimental load-time responses ($NRMS$ errors: 0.072, 0.102, and 0.107 for 1.5 m/s, 3.0 m/s, and 5.0 m/s). Optimised parameters are detailed in Table II. The quasi-static elastic modulus and yield stress of cortical bone range from 7.5 GPa to 19.3 GPa and from 63 MPa to 118 MPa, respectively.

TABLE II
DESIGN PARAMETERS, THEIR RANGES AND THEIR OPTIMISED VALUES OBTAINED FROM INVERSE FE OPTIMISATION

Material parameters	Equation		Design parameter	Range		Optimised value
Quasi-static elastic modulus	$E_0 = \boldsymbol{a}\rho^{\boldsymbol{b}}$	(3)	a b	1.0 0.1	12 2.5	9.76 0.98
Strain-rate-dependent elastic modulus	$E = \frac{1}{2}E_0\left(1+\boldsymbol{B_1}^{log\left(\frac{\dot{\varepsilon}}{\dot{\varepsilon}_0}\right)}\right)$	(4)	B_1	0.5	1.5	1.32
Quasi-static yield stress	$\sigma_{y0} = \boldsymbol{c}\rho^{\boldsymbol{d}}$	(5)	c d	0.01 0.1	0.1 2.5	0.08 0.64
Strain-rate-dependent yield stress	$\sigma_y = \frac{1}{2}\sigma_{y0}\left(1+\boldsymbol{B_2}^{log\left(\frac{\dot{\varepsilon}}{\dot{\varepsilon}_0}\right)}\right)$	(6)	B_2	0.5	1.5	0.62
Tangent modulus	$E_t = \boldsymbol{t} \times E$	(7)	t	0.001	0.10	0.047

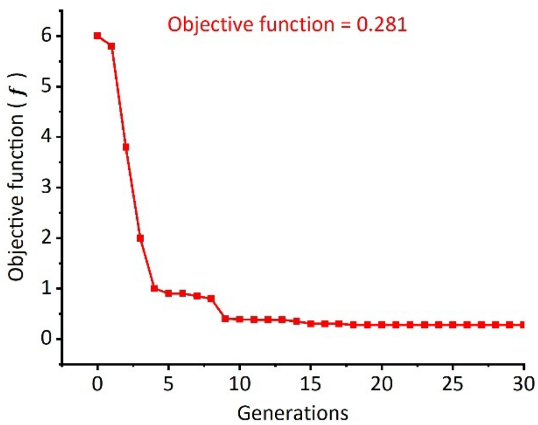

Fig. 3. GA Convergence plot.

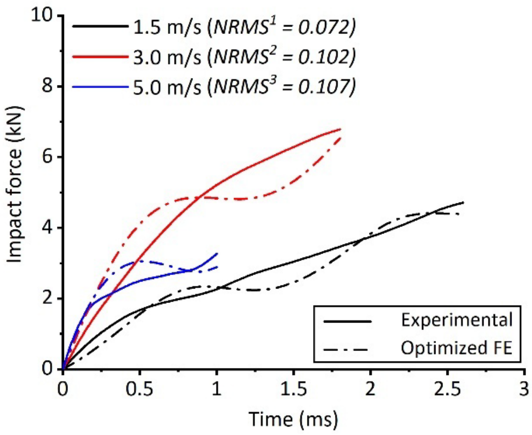

Fig. 4. Experimental and optimised force-time response.

IV. DISCUSSION

The peak load at failure was lowest at an impact velocity of 5.0 m/s, which could be due to the density of the specimen or to its geometric characteristics. The inertial moment (Iz) of the cross-section at the fracture site significantly influences the bone's structural response under three-point bending [17]. CT-derived Iz values, computed using a custom MATLAB script, indicate a lower Iz for the femur tested at 5.0 m/s compared to other specimens.

Cortical bone behaviour, including material orthotropy, compression-tension asymmetry and complex failure processes, is not fully represented in the current model. Additionally, fracture initiation and propagation are not simulated. Future improvements are required to address these aspects while balancing the number of design parameters and the computational efficiency.

V. CONCLUSION

The present study characterised the structural response of the human femur under dynamic three-point bending loads. The material model parameters of the strain-rate-dependent model were optimised through the experimental force-time response utilising a genetic algorithm-based inverse FE characterisation. The simulation results demonstrate a reasonable agreement with the experimental load-time responses, with the greatest $NRMS$ error across all impact velocities being 0.107. Further improvements in the material model are required to incorporate fracture initiation and propagation simulation functionalities.

VI. ACKNOWLEDGEMENTS

The authors acknowledge the financial support received from the DRDO Industry Academia Centre of Excellence, IIT Delhi (DFTM/03/3203/M/01/JATC).

VII. REFERENCES

[1] Newton, E. J. and Love, J. (2007) Emergency Department Management of Selected Orthopedic Injuries. *Emergency Medicine Clinics of North America*, **25**(3): pp. 763–793.
[2] Lee, K. M., Lee, S. Y., Han, C. S., Choi, S. M. (2020) Long bone fracture type classification for limited number of CT data with deep learning. *Proceedings of the ACM Symposium on Applied Computing,* 2020, Brno, Czech Republic.
[3] Sachse, D., Bludau, F., Obertacke, U. (2010) Fractures of the neck of the femur in younger patients (15-50 years old): Systematic literature research on medial fractures of the neck of the femur in young patients. Schenkelhalsfrakturen bei Jüngeren Patienten (15-50 Jahre): *Systematische Literaturre. Unfallchirurg*, **113**(1): pp. 69–74.
[4] Singaram, S. and Naidoo, M. (2019) The physical, psychological and social impact of long bone fractures on adults: A review. *African Journal of Primary Health Care and Family Medicine*, **11**(1).
[5] Abdel-Wahab, A. A. and Silberschmidt, V. V. (2011) Dynamic properties of cortical bone tissue: Impact tests and numerical study. *Applied Mechanics and Materials*, **70**: pp. 387–392.
[6] Fleps, I., Guy, P., Ferguson, S. J., Cripton, P. A., Helgason, B. (2019) Explicit Finite Element Models Accurately Predict Subject-Specific and Velocity-Dependent Kinetics of Sideways Fall Impact. *Journal of Bone and Mineral Research*, **34**(10): pp. 1837–1850.
[7] Iwamoto, M., Miki, K., Tanaka, E. (2005) Ankle Skeletal Injury Predictions Using Anisotropic Inelastic Constitutive Model of Cortical Bone Taking into Account Damage Evolution. *SAE Technical Papers* (November): pp. 133–156.
[8] Helgason, B., Perilli, E., *et al*. (2008) Mathematical relationships between bone density and mechanical properties: A literature review. *Clinical Biomechanics*, **23**(2): pp. 135–146.
[9] Schileo, E., Taddei, F., Malandrino, A., Cristofolini, L., Viceconti, M. (2007) Subject-specific finite element models can accurately predict strain levels in long bones. *Journal of Biomechanics*, **40**(13): pp. 2982–2989.
[10] Eberle, S., Göttlinger, M., Augat, P. (2013) An investigation to determine if a single validated density-elasticity relationship can be used for subject-specific finite element analyses of human long bones. *Medical Engineering and Physics*, **35**(7): pp. 875–883.
[11] Pakdel, A., Fialkov, J., Whyne, C. M. (2016) High-resolution bone material property assignment yields robust subject-specific finite element models of complex thin bone structures. *Journal of Biomechanics*, **49**(9): pp. 1454–1460.
[12] Arun, M. W. J., Chawla, A., Mukherjee, S. (2011) Predicting fracture initiation, propagation and diversion in long bones under impact using Drucker-Prager plastic model and damage modeling. American society of biomechanics, 2011, Long Beach, California, USA.
[13] Malik, A., Yadav, V. V., Chawla, A., Datla, N. V. (2023) Predicting Impact Response of Human Femur using Material Mapping Strategy. 28th Congress of the European Society of Biomechanics, 2023, Maastricht, The Netherlands.
[14] Linde, F., Hvid, I., Pongsoipetch, B. (1989) Energy absorptive properties of human trabecular bone specimens during axial compression. *Journal of Orthopaedic Research*, **7**(3): pp. 432–439.
[15] Li, Z., Wang, J., *et al*. (2020) Experimental and numerical study on the mechanical properties of cortical and spongy cranial bone of 8-week-old porcines at different strain rates. *Biomechanics and Modeling in Mechanobiology*, **19**(5): pp. 1797–1808.

[16] Enns-Bray, W. S., Bahaloo, H., *et al*. (2018) Material mapping strategy to improve the predicted response of the proximal femur to a sideways fall impact. *Journal of the Mechanical Behavior of Biomedical Materials*, **78**: pp. 196–205.
[17] Du, X., Jiang, B., Zhang, G., Chou, C. C., Bai, Z. (2021) Study on the Long Bone Failure Behaviors under the Indenter Rigid-Contact by Experiment Analysis and Subject-Specific Simulation. *Journal of Biomechanical Engineering*, **143**(2): 021003.